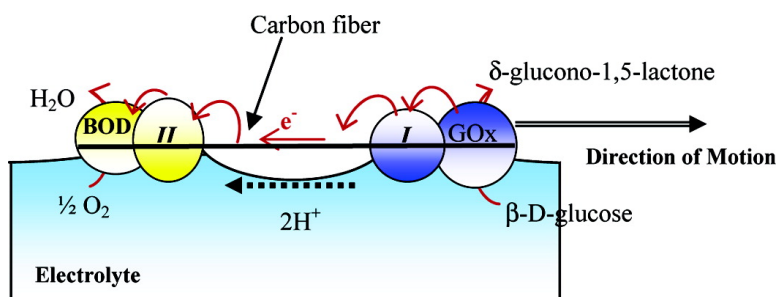


Bioelectrochemical Propulsion

Nicolas Mano, and Adam Heller

J. Am. Chem. Soc., **2005**, 127 (33), 11574-11575 • DOI: 10.1021/ja053937e • Publication Date (Web): 28 July 2005

Downloaded from <http://pubs.acs.org> on March 25, 2009



More About This Article

Additional resources and features associated with this article are available within the HTML version:

- Supporting Information
- Links to the 18 articles that cite this article, as of the time of this article download
- Access to high resolution figures
- Links to articles and content related to this article
- Copyright permission to reproduce figures and/or text from this article

[View the Full Text HTML](#)

Bioelectrochemical Propulsion

Nicolas Mano* and Adam Heller

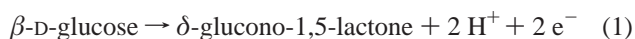
Department of Chemical Engineering and Texas Materials Institute, The University of Texas at Austin, Austin, Texas 78712

Received June 14, 2005; E-mail: mano@mail.utexas.edu

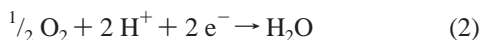
Biological locomotion by protein-based molecular machines, powered by reactions of energy-rich molecules, such as ATP, abounds in nature.^{1–3} The design of man-made machines in which chemical energy is directly converted to mechanical energy, utilized in their propulsion, is one of the challenges of contemporary bioengineering.⁴ Locomotion by the reaction of glucose and oxygen has not been previously reported. Here, we show that a carbon fiber is propelled rapidly at the water–O₂ interface when built with a terminal glucose oxidizing microanode and an O₂ reducing microcathode. The flow of current through the fiber is accompanied by transport of ions, which is so fast at the interface, where the viscous drag is small, that it carries the fiber at ~1 cm s⁻¹.

Earlier, small objects, of micrometer to millimeter size, have been chemomechanically propelled by the gaseous O₂ evolved in the platinum-catalyzed decomposition of hydrogen peroxide (2H₂O_{2(l)} → O_{2(g)} + 2 H₂O_{2(l)}).^{5–9} Macroscopic hemicylindrical poly(dimethyl siloxane) plates, having a platinized domain,⁶ were propelled by the recoil when the O₂ bubbles departed from their catalyst surface. Microscopic (2 μm long, 370 nm diameter) platinum–gold rods were shown to move autonomously in aqueous H₂O₂ along an interfacial tension gradient,⁷ and the direction of the motion of Ni–Au–Ni–Au nanorods in H₂O₂ solution was controlled by an applied magnetic field.⁸ Self-powered nanomotors have been formed with bar-coded gold–nickel nanorods, their gold end anchored to the surface of a silicon wafer;⁵ some had a gear-like gold structure with platinum deposited on the teeth of the gears.⁹

In the direct bioelectrochemical to mechanical power conversion process of this communication, conductive carbon fibers, of 0.5–1 cm length and 7 μm diameter, were autonomously propelled by the glucose–oxygen reaction at 37 °C and at pH 7 under 1 atm O₂. The fibers had central 4–8 mm long hydrophobic segments, making them float at the solution–gas interface (Scheme 1A). Their ~1 mm long bioelectrocatalyst-coated end-segments were, however, hydrophilic and in electrolytic contact with the solution. One of their end-segments was coated with a bioelectrocatalyst for the oxidation of glucose, redox polymer wired glucose oxidase (GOx).¹⁰ Their opposite end-segment was coated with a bioelectrocatalyst for the four-electron reduction of O₂ to water, redox polymer wired bilirubin oxidase (BOD).¹¹ In the resulting electrically shorted biofuel cell, the anode reaction was



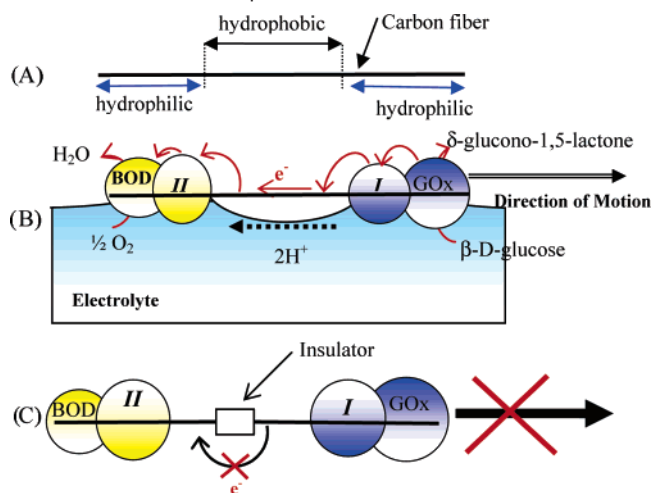
and the cathode reaction was



resulting in the net bioelectrochemomechanical power-generating reaction



Scheme 1. The Self-Propelled Bioelectrochemical Motor^a



^a (A) The two ends of a carbon fiber are made hydrophilic by exposure to a 1 Torr O₂ plasma. (B) One end of the fiber is modified with the electrostatic adduct of glucose oxidase (GOx) and redox polymer *I*. The other end is modified with an electrostatic adduct of bilirubin oxidase (BOD) and redox polymer *II*. When the fiber is dipped in a pH 7 buffer solution containing 10 mM glucose, electrons flow along the path glucose → GOx → *I* → carbon fiber → *II* → BOD → O₂, and the fiber is propelled at the solution–O₂ interface by the ion flow accompanying the flow of electrons. (C) When an insulator is introduced between the two electrocatalytic fiber ends, the fiber does not move.

In the absence of glucose under 1 atm O₂ or in the presence of glucose, but under 1 atm N₂, the fibers were still (Movie 1, Supporting Information). In the presence of glucose and O₂, an electron current flowed from the glucose anode to the O₂ cathode through the carbon fiber. This current was balanced by a stream of ions, hydrated protons, flowing at/or near the gas–solution interface from the anode to the cathode, propelling the fibers (Scheme 1B).

When the GOx/BOD ratio was balanced for approximately similar reaction rates at the two fiber ends, the trajectory of the fibers was linear. The fibers were propelled at a velocity of ~1 cm s⁻¹ for 20 s, their velocity decreasing to ~0.1 cm s⁻¹ after ~1 min, and the fibers halted after ~3 min (Movie 2, Supporting Information; snapshot series of Figure 1A). When, a small excess of GOx was applied, the trajectory of the fibers was spiral (Movie 3, Supporting Information; snapshot series of Figure 1B). At a large excess of GOx, the fibers rotated around their anode (Movie 4, Supporting Information; snapshot series of Figure 1C) at ~5 revolutions/s (rps) for ~5 s, with their rotation decreasing after 10 s to ~2 rps and halting after 2 min. After a fiber halts, a fresh fiber does not move in the solution in which the fiber halted, showing that halting and solution contamination are associated. Adding 40 mg/mL of either glucose oxidase or bilirubin oxidase, which would form like most proteins, a monolayer at the interface, caused the fibers to be still.

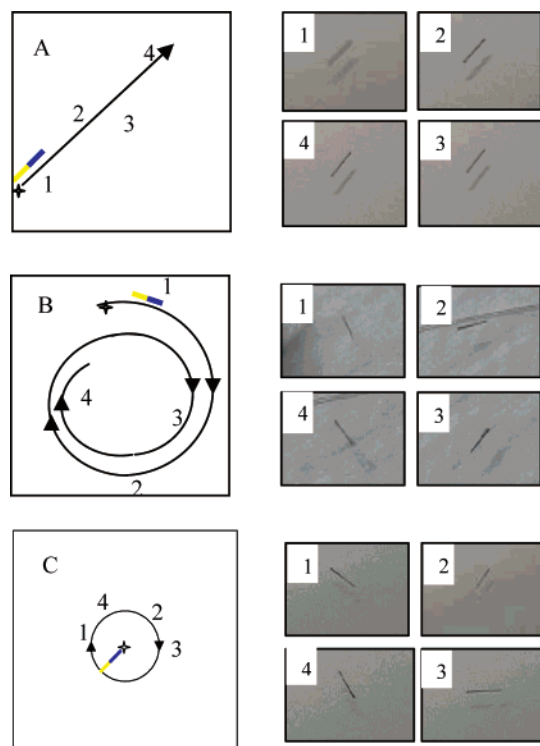


Figure 1. Graphs and images illustrating the motion. (A) Top left at $\text{GOx/BOD} \sim 1$, the trajectory is linear. Right: pictures taken at $t = 0.2$ s (1), $t = 3$ s (2), $t = 5$ s (3), and $t = 8$ s (4). (B) Left: when $\text{GOx/BOD} > 1$, the trajectory is spiral. Right: pictures taken at $t = 0.2$ s (1), $t = 1$ s (2), $t = 3.8$ s (3), and $t = 6$ s (4). (C) Left: when $\text{GOx/BOD} \gg 1$, rotation around the anode is observed (blue). Right: pictures taken at $t = 1$ s (1), $t = 7$ s (2), $t = 10$ s (3), and $t = 16$ s (4).

Electron conduction by the fibers was necessary for locomotion. Fibers comprising two insulating epoxy-bonded segments were still (Scheme 1C). The mere presence of GOx and BOD was insufficient for propulsion; there was no movement when the electrons could not flow from the anode to the cathode. Furthermore, only hydrophobic fibers, residing at the water–gas interface, not fully immersed in the solution, were visibly propelled. When made hydrophilic by exposure to a low-pressure O_2 plasma, they were fully immersed and still. The velocities of the floating fibers were sensitive to the ionic strength, increasing as the concentration of the $\text{NaH}_2\text{PO}_4\text{--Na}_2\text{HPO}_4$ electrolyte was decreased from 1 M to 10 mM. They were also sensitive to the glucose concentration, increasing as the glucose concentration was increased from 2 to 32 mM.

The oxidation of glucose and the reduction of O_2 result in a pH gradient (reactions 1 and 2). We propose that protons and their associated water molecules flow from the anode to the cathode in this pH gradient, their stream carrying the floating fibers. The hydrated proton stream is rapid, and the fibers move, only where the viscous drag is small, at the gas–water interface. Thermodynamically, it is the difference in the concentration of ions (in this case, hydrated protons) at the gas–water interface, translating to a difference in the surface tensions between the anode and near the cathode,¹² that underlies the surface-pressure gradient creating the fast flow.

The model explains most of the experimental observations; in the absence of either glucose or oxygen, or if the circuit is resistive because the anode is electrically insulated from the cathode, a propulsion-driving ion concentration (pH) gradient does not exist. When a protein is added, the fiber is wetted, submersed, and no movement is observed because of the expectedly increased viscous drag, which is far greater in the solution than at its surface. The movement is now too slow to be seen by the naked eye. Leaching of one of the enzymes, which like all proteins are surface-active, slows, then stops the movement. Increase in ionic strength not only affects the surface tension, lessening the difference between the tensions at the anode and the cathode, but also slows the kinetics of glucose electrooxidation and O_2 electroreduction through phase separation of the electrostatic adduct of the enzyme and its polymeric wires.^{13,14} We are still searching for the cause of the dependence of the trajectory on the excess GOx.

In summary, we report locomotion, powered by the reaction of glucose and oxygen, and show that power generated in a bioelectrochemical reaction can be directly converted to propulsive mechanical power.

Acknowledgment. The study was supported by the Office of Naval Research (N00014-02-1-0144) and by the Welch Foundation. N.M. thanks The Oronzio de Nora Industrial Electrochemistry Fellowship of The Electrochemical Society.

Supporting Information Available: Four movies showing the motion of fibers (1) in the absence of glucose, under 1 atm O_2 , and in the presence of glucose, but under 1 atm N_2 , where the fiber is still; (2) for $\text{GOx/BOD} \approx 1$, where the trajectory is straight, the fiber propelled at a velocity of ~ 1 cm s^{-1} ; (3) for $\text{GOx/BOD} > 1$, where the trajectory is spiral; and (4) for $\text{GOx/BOD} \gg 1$, where the fiber rotates. This material is available free of charge via the Internet at <http://pubs.acs.org>.

References

- (1) Soong, R. K.; BachAnd, G. D.; Neves, H. P.; Olkhovets, A. G.; Montemagno, C. D. *Science* **2000**, *290*, 1555–1558.
- (2) Nedelec, F. J.; Surrey, T.; Maggs, A. C.; Leibler, S. *Nature* **1998**, *389*, 305–308.
- (3) Alberts, B. *Cell* **1998**, *92*, 291–294.
- (4) Yin, P.; Yan, H.; Daniell, X. G.; Turbefeild, A. J.; Reif, J. H. *Angew. Chem., Int. Ed.* **2004**, *43*, 4906–4911.
- (5) Fournier-Bidoz, S.; Arsenaault, A. C.; Manners, I.; Ozin, G. A. *Chem. Commun.* **2005**, 441–443.
- (6) Ismagilov, R. F.; Schwartz, A.; Bowden, N.; Whitesides, G. M. *Angew. Chem., Int. Ed.* **2002**, *41*, 652–654.
- (7) Paxton, W. F.; Kistler, K. C.; Olmeda, C. C.; Sen, A.; St. Angelo, S. K.; Cao, Y.; Mallouk, T. E.; Lammert, P. E.; Crespi, V. H. *J. Am. Chem. Soc.* **2004**, *126*, 13424–13431.
- (8) Kline, T. R.; Paxton, W. F.; Mallouk, T. E.; Sen, A. *Angew. Chem., Int. Ed.* **2005**, *44*, 744–746.
- (9) Catchmark, J. M.; Subramanian, S.; Sen, A. *Small* **2005**, *1*, 202–206.
- (10) Mao, F.; Mano, N.; Heller, A. *J. Am. Chem. Soc.* **2003**, *125*, 4951–4957.
- (11) Mano, N.; Kim, H.-H.; Zhang, Y.; Heller, A. *J. Am. Chem. Soc.* **2002**, *124*, 6480–6486.
- (12) Manciu, M.; Ruckenstein, E. *Adv. Colloid Interface Sci.* **2003**, *105*, 63–101.
- (13) Heller, A. *J. Phys. Chem.* **1992**, *96*, 3579–3587.
- (14) Mano, N.; Fernandez, J. L.; Kim, Y.; Shin, W.; Bard, A. J.; Heller, A. *J. Am. Chem. Soc.* **2003**, *125*, 15290–15291.

JA053937E